AMSI VACATION RESEARCH SCHOLARSHIPS 2019–20

EXPLORE THE MATHEMATICAL SCIENCES THIS SUMMER

Global Sensitivity Analysis of a Model for Cyprinid Herpes Virus 3 as a Biocontrol Agent of Common Carp

Stephanie Fuser

Supervised by A/Prof Stephen Davis

RMIT University

Vacation Research Scholarships are funded jointly by the Department of Education and the Australian Mathematical Sciences Institute.

AMSI AUSTRALIAN MATHEMATICAL SCIENCES INSTITUTE

Australian Government Department of Education

Abstract

Common carp (*Cyprinus carpio*) dominate freshwater systems is southeastern Australia; decreasing water quality and adversely effecting native fish populations. The Australian Government have proposed the use of Cyprinid Herpes Virus 3 (CyHV-3) as a biocontrol measure to reduce carp numbers below levels known to cause environmental harm. In this report we have developed three epidemiological models to describe the dynamics of the spread of CyHV-3 within a naïve carp population. The base model simulates disease progression through a single, well-mixed population with simple demographic processes. The model was also extended by including water temperature dependent viral transmission and exploring transmission between age classes. A global sensitivity analysis was conducted on the base model and seasonal model to identify how dependent the resultant population is to particular parameter inputs. The key finding of the study was that the sensitivity analysis revealed that the case fatality rate is considerably the biggest driver for explaining the variance in the reduction of the population size. This suggests further exploration is required to understand the ancestry of Australian carp as genetic resistance may have future impacts. The results also showed that increasing bio-complexity to the model did not change the outcome of the global sensitivity analysis.

1 Introduction

The deliberate release of Cyprinid Herpes Virus 3 (CyHV-3) to control invasive common carp (*Cyprinus carpio*) in the Murray-Darling Basin of south-eastern Australia is highly controversial (Hanifie, 2020). Carp are considered an invasive pest in Australia, where their impacts are felt environmentally, economically and socially, and where they are not considered valuable as either a sport fish or as a food source. The Australian Government has since funded an extensive research program to assess the viability of biocontrol to reduce carp density to levels that are not considered harmful to water quality or native fish (Williams et al., 2002; Parkos et al., 2003; Haas et al., 2007; Matsuzaki et al., 2009). The proposed biocontrol agent CyHV-3 is a strain of herpes which infects common carp and is naturally present in the northern hemisphere. It has had immense impacts on wild and farmed carp populations across Europe, the USA and Japan, and causes mortality in the majority of infected fish. The proposed use of the virus is controversial because scientists have

raised concerns about the effectiveness and costs associated with a deliberate release, and the possibility that the virus might do more ecological harm than good (Hanifie, 2020).

A complex mathematical model for CyHV-3 in common carp populations (Davis et al., 2020) has been developed to counter: (i) the lack of epidemiological data on epidemics in wild carp populations; and (ii) the inability to undertake controlled field trials without a high risk of the virus inadvertently spreading. In this study we have first considered a much simpler version of the epidemiological model where carp are treated as a single, well-mixed population of hosts. While simple models such as these are not appropriate to make specific predictions about the impact of CyHV-3, they can reveal the range of dynamics and outcomes that might be expected following release into a naïve population. We have also extended the model and added greater biological realism by including seasonality in carp recruitment and virus transmission; and investigated virus transmission between different age classes.

The objective of this study is to identify which parameters in the model have the greatest effect on the resultant host population size following introduction of CyHV-3. We achieve this by conducting a global sensitivity analysis on the simple and extended models.

1.1 Statement of Authorship

The workload was divided as follows:

- Stephanie Fuser developed the R code to run the model and sensitivity analysis, produced graphs and figures, reported and interpreted the results, and wrote this report.
- A/Prof Stephen Davis developed the epidemiological model, supervised the project and proofread this report.

2 Mathematical Model

2.1 Base Model

In this first model of CyHV-3 individual carp progress through five different disease states. All individuals are initially susceptible (S), but upon contact with (released) carp that are infectious they transition to an exposed state (E). During this time, known as the incubation period, the virus replicates within the host until it reaches a critical point where the carp becomes infectious to others. It is expected that once carp have progressed to an infectious state (I), ~80% will die due to the virus (McColl et al, 2017). Surviving carp become chronically infected (L) where the virus

remains latent until reactivation of the virus causing the carp to become re-infectious. Subsequently, secondarily infectious carp (Z) can once more become latent and the cycle continues (see Figure 1).

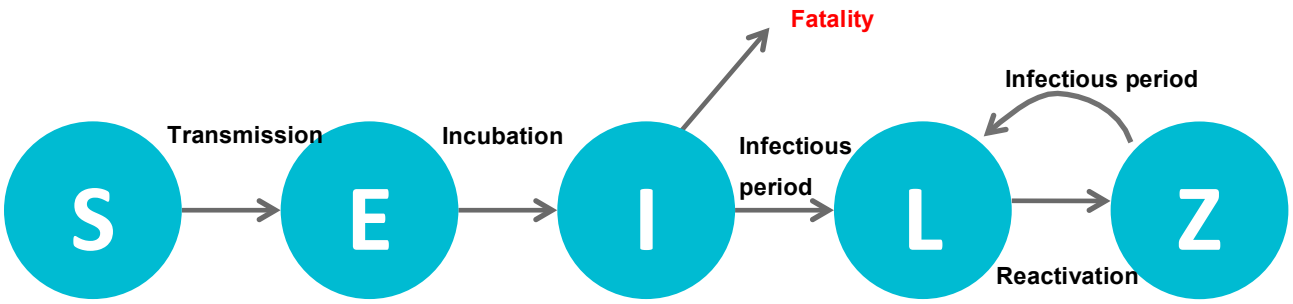

Figure 1 Conceptual representation of carp disease states: Susceptible (S), Exposed (E), Infectious (I), Chronically Infected (L) and Secondarily Infected (Z)

2.1.1 Governing Equations

Parameterization of the rates at which individual hosts transition between the states lead to the following governing system of differential equations is:

$$\frac{dS}{dt} = B - \beta S(I + Z) - \mu S$$

$$\frac{dE}{dt} = \beta S(I + Z) - \eta E - \mu E$$

$$\frac{dI}{dt} = \eta E - \gamma I - \mu\gamma$$

$$\frac{dL}{dt} = (1 - f1)\gamma I + \gamma Z - \sigma L - \mu L$$

$$\frac{dZ}{dt} = \sigma L - \gamma Z - \mu Z$$

Parameters

N	Total population size
μ	Natural mortality rate
B	Births per day
β	Transmission rate
1/η	Incubation period
1/γ	Infectious period
f1	Fatality rate
1/σ	Latent period

Since we wish to measure the impact of CyHV-3 on carp over a time scale of years to decades we cannot assume that the population is closed (i.e. no births or deaths) and we must include the recruitment of new susceptible hosts (births). In this case we assume a natural, background per capita mortality rate, and then set the birth rate to be a fixed constant rate independent of the population size. This leads to a simple equation for the number of hosts at equilibrium when no infectious agent is released into the population,

$$N^* = \frac{B}{\mu}$$

i.e. the population settles to a constant size. In practice we allow $N^*$to vary and set B.

2.2 Seasonal Model

The base model was next extended where we have focused on the efficacy of CyHV-3 transmission given seasonal dynamics of water temperature. It is inferred from observational records that expected outbreaks occur in spring (Uchii et al. 2014). This is thought to coincide with permissive water temperatures and the reproductive behaviour of carp (mass spawning events which occur in spring) where the chance of contact is greater. Experimental data have concluded that viral transmission occurs within a permissive range between 16°C and 28°C (Yuasa et al. 2008), where within this range we expect disease progression and shedding of virus and thus viral outbreaks.

In this model we have assumed that viral transmission within the permissive range will be constant (β_c). At times of the year when water temperatures are outside of this range then we have assumed all transmission will cease. To simulate this "on/off switch" of viral replication we have used a Heaviside step function as shown in equation (2), which is dependent on a sinusoidal model of yearly water temperatures (1).

$$\boldsymbol{Temperature = a - bcos\left(\frac{2\pi t}{365}\right)} \qquad \textbf{(1)}$$

$$\boldsymbol{\beta(T) = [H(T-16) - H(T-28)]\beta_c} \qquad \textbf{(2)}$$

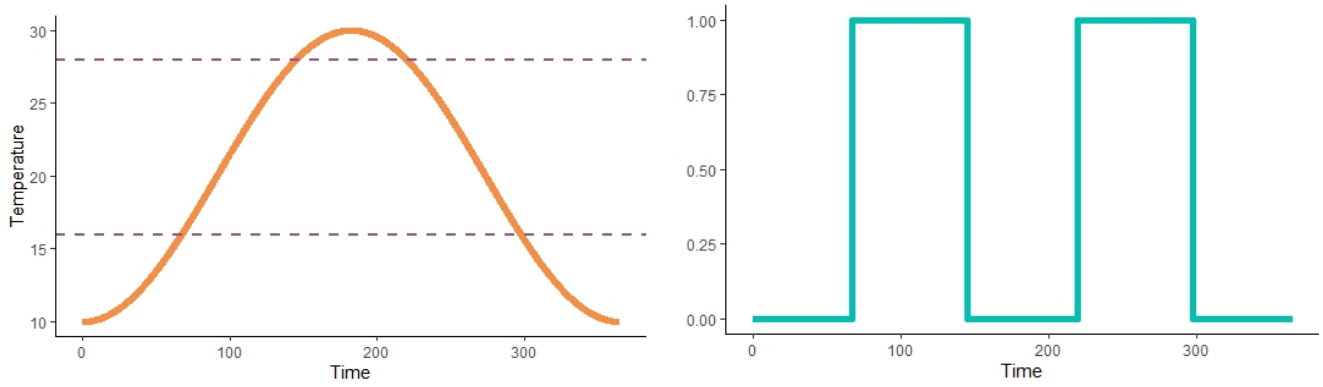

Figure 2 Water temperature over one year starting from 1st July (orange). The purple dotted lines represent the extremes of the permissive range for viral transmission (between 16°C and 28°C). The step function in blue highlights when the virus is on or off according to the permissive range.

2.3 Age Structured Model

Lastly, we extended the model by including a simple form of age structure. The risk of infection between carp is likely to be dependent on age/size. Eggs and larvae (0-3 weeks) are known to have no to little risk of viral infection, however carp older than 3 weeks are considered susceptible (Davis et al., 2020). For simplicity, we have subdivided the host population into just two age classes (juvenile and adult) where reproduction only occurs within the adult population.

Infected juveniles will be introduced to carp populations to initiate virus outbreaks. As shown in figure 3, there are now 10 state variables (5 disease states x 2 age-classes). The disease progression is the same for each age class but there is now a rate of maturation of juvenile carp to adult carp, which we assume happens independently of disease state.

We can now expect that viral propagation can occur amongst and between members of both age classes, but that this will happen at different rates. In the below transition matrix, we assume that the juvenile-to-juvenile contact rate is an order of magnitude lower than the adult-to-adult contact rate and the contact rates between the two classes (adult-to-juvenile and juvenile-to-adult) are equal and another order of magnitude less than the adult-to-adult contact rate. This will capture the seasonal aggregation of adult carp during spring reproduction where we assume that viral transmission is greatest between adult-to-adult contact.

$$\boldsymbol{\beta} = \begin{bmatrix} \boldsymbol{\beta_{jj}} & \boldsymbol{\beta_{ja}} \\ \boldsymbol{\beta_{aj}} & \boldsymbol{\beta_{aa}} \end{bmatrix} = \begin{bmatrix} \mathbf{0.1}\boldsymbol{\beta_{aa}} & \mathbf{0.01}\boldsymbol{\beta_{aa}} \\ \mathbf{0.01}\boldsymbol{\beta_{aa}} & \boldsymbol{\beta_{aa}} \end{bmatrix} \qquad \textbf{(3)}$$

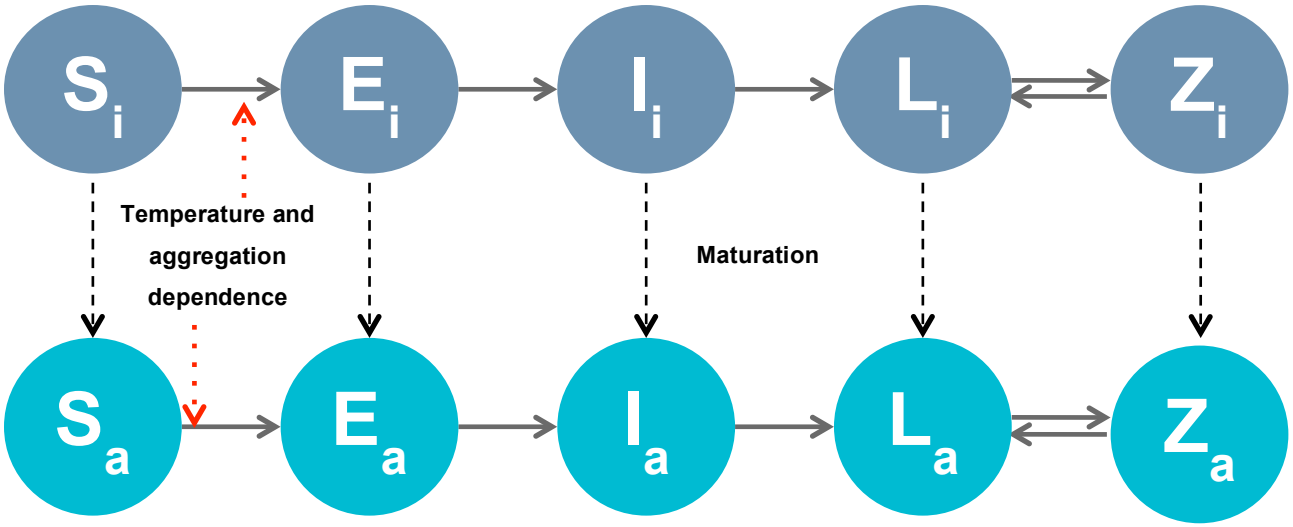

Figure 3 Conceptual flow diagram of disease states between two different age-classes, where there is maturation from juveniles (j) to adults (a).

2.3.1 Governing Equations

Our assumptions lead to the following system of differential equations where the two age classes – Juvenile and Adult - are identified by subscripts j and a,

$$\frac{dS_j}{dt} = B - S_j[\beta_{jj}(I_j + Z_j) + \beta_{ja}(I_a + Z_a)] - \mu S_j - \varphi S_j$$
$$\frac{dE_j}{dt} = S_j[\beta_{jj}(I_j + Z_j) + \beta_{ja}(I_a + Z_a)] - \eta E_j - \mu E_j - \varphi E_j$$
$$\frac{dI_j}{dt} = \eta E_j - \gamma I_j - \mu I_j - \varphi I_j$$
$$\frac{dL_j}{dt} = (1 - f1)\gamma I_j + \gamma Z_j - \sigma L_j - \mu L_j - \varphi L_j$$
$$\frac{dZ_j}{dt} = \sigma L_j - \gamma Z_j - \mu Z_j - \varphi Z_j$$

$$\frac{dS_a}{dt} = -S_a[\beta_{aa}(I_a + Z_a) + \beta_{aj}(I_j + Z_j)] - \mu S_a + \varphi S_a$$
$$\frac{dE_a}{dt} = S_a[\beta_{aa}(I_a + Z_a) + \beta_{aj}(I_j + Z_j)] - \eta E_a - \mu E_a + \varphi E_a$$
$$\frac{dI_a}{dt} = \eta E_a - \gamma I_a - \mu I_a + \varphi I_a$$
$$\frac{dL_a}{dt} = (1 - f1)\gamma I_a + \gamma Z_a - \sigma L_a - \mu L_a \mp \varphi L_a$$
$$\frac{dZ_a}{dt} = \sigma L_a - \gamma Z_a - \mu Z_a + \varphi Z_a$$

The transmission rate (β_{xx}) remains temperature dependent and is modelled with the step function as described in (2).

φ denotes the maturation rate of juvenile carp to adult carp.

2.4 Model Outputs

In order to interpret results from the models and sensitivity analysis, this research focuses on two model outputs:

1. The peak (maximum) fraction of hosts infected. This is significant since an outbreak may cause a large number of deaths in a small timeframe, and hence there may be consequences for water quality.

2. Population suppression – the number of carp after virus release relative to the number of carp had the virus not been released.

3 Global Sensitivity Analysis

A global sensitivity analysis (GSA) is the process of how uncertainty in the model output can be apportioned to the uncertainty in model input factors (Saltelli et al., 2010).

3.1 Sobol's Indices

Sobol's indices were used for the GSA; this is a variance-based method that produces two indices that capture first order and total effects of parameter variation on model output. The first order index S_i is the proportion of the variance in the model output that is attributed to the variance in factor X_i:

$$S_i = \frac{Var_{X_i}[E_{X_{\sim i}}(Y|X_i)]}{Var(Y)},$$

where X_i is the i-th factor and $X_{\sim i}$ represents all factors excluding X_i. The expected value of output Y is determined by fixing X_i and varying values for $X_{\sim i}$. The variance of expected values over a distribution of different X_i produce the numerator to this equation. Since this is a proportion of the total variance in Y, we expect S_i to be between zero and one.

Higher order indices (e.g $S_{1,2}$) can also be calculated by fixing multiple factors at a time. This index shows us the variance in the model output due to the fixed factors interacting. We did not calculate the higher order indices because that is computationally expensive. In this

circumstance, the total effect was measured. The total effect index takes into account the direct contribution (S_i) and all interaction effects,

$$S_{Ti} = \frac{E_{X_{\sim i}}[Var_{X_i}(Y|X_{\sim i})]}{Var(Y)} = 1 - \frac{Var_{X_{\sim i}}[E_{X_i}(Y|X_{\sim i})]}{Var(Y)}.$$

3.2 Parameter Space

Since the model is a black box simulation, which means the model deterministically generates outputs based on inputs, the only randomness involved is in the selection of the input parameters. The parameters are randomly generated within a parameter space established from point estimates of parameters.

	Parameter	Point Estimate	Reference/Notes	Minimum	Maximum
Initial population size	N	1,000	Arbitrarily chosen- not enough information on this value	100	10,000
Natural mortality rate	μ	1/365	Arbitrarily chosen- no information on this value	1/730	2/365
Birth rate	B	Nμ	See 2.1.1	-	-
Transmission rate	β_a	0.001	Arbitrarily chosen- no information on this value	0.0001	0.01
Incubation period	1/η	2 days	Omori & Adams (2011); unpublished data (Davis et al., 2020)	1 day	3 days
Infectious period	1/γ	5 days	Omori & Adams (2011)	2 days	10 days
Fatality rate	f1	0.8	McColl et al (2017)	0.5	0.9
Latent period	1/σ	1000 days	Arbitrarily chosen. There is no information on this parameter, but reactivation was assumed to be rare	100 days	10,000 days

Maturation period	1/φ	60 days	Fao.org (2020)	1/120	1/30
Minimum average temperature	MinT	10°C	unpublished data (Davis et al., 2020)	8°C	13°C
Maximum average temperature	MaxT	28°C	unpublished data (Davis et al., 2020)	26°C	31°C

Table 1 Parameter space (maximum and minimum) used to generate parameter values used to calculate Sobol's indices.

4 Results

4.1 Peak Infection

Due to time constraints and computer limitations, a global sensitivity analysis of the peak infection was only conducted for the base model and seasonal model. Comparing the GSA of both models (figure 4) there appears to be no significant difference between the two. Gamma had the greatest main effect and total effect index. The total effect of gamma is slightly higher than the main effect signifying that there is little interaction with other parameters and that gamma has a direct effect on the infectious peak. This proves acceptable since gamma captures the infectious period. Beta (transmission rate) and N (population size) both have an effect on the peak and since the difference between the total effect index and main effect index of each parameter appear similar it can be assumed they are interacting parameters. This is also expected since beta and N are parameters within the nonlinear part of the differential equations for the model. Eta is concerned with the incubation period of CyHV-3, so it is anticipated that it will have an effect on the maximum fraction of hosts infected. Water temperatures were shown to have no influence on the output variance.

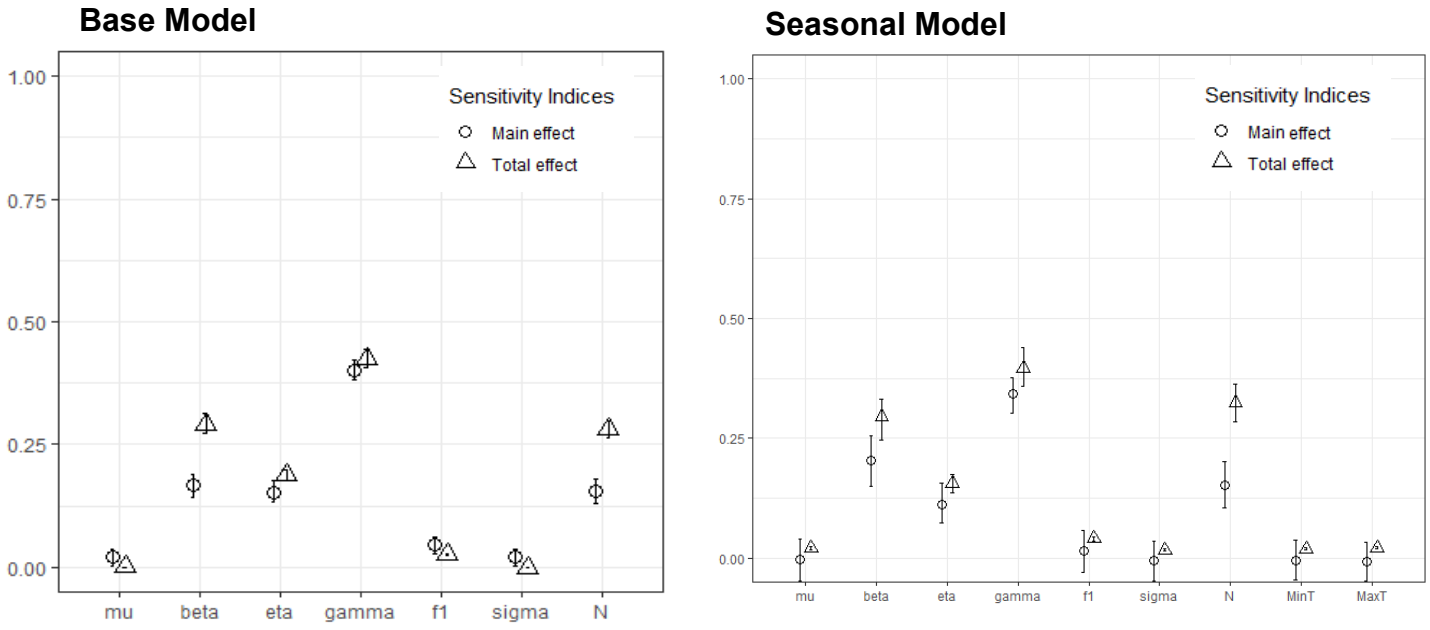

Figure 4 Global sensitivity analysis for base model (left) and seasonal model (right) of peak infection as a model output

4.2 Population Suppression

Once more, the GSA for each model was very similar, as shown in figure 5. However, unlike the previous model output, the GSA for population suppression has a distinct parameter that can explain variance within the model. f1 (fatality rate) had overwhelmingly greater indices compared to the other parameters, indicating it is the main driver of population reduction. Transmission rate and population size had an effect on the model output and again appear to interact. These parameters seem to be important for the occurrence of an epidemic since it influences the rate in which susceptible individuals are exposed to the virus.

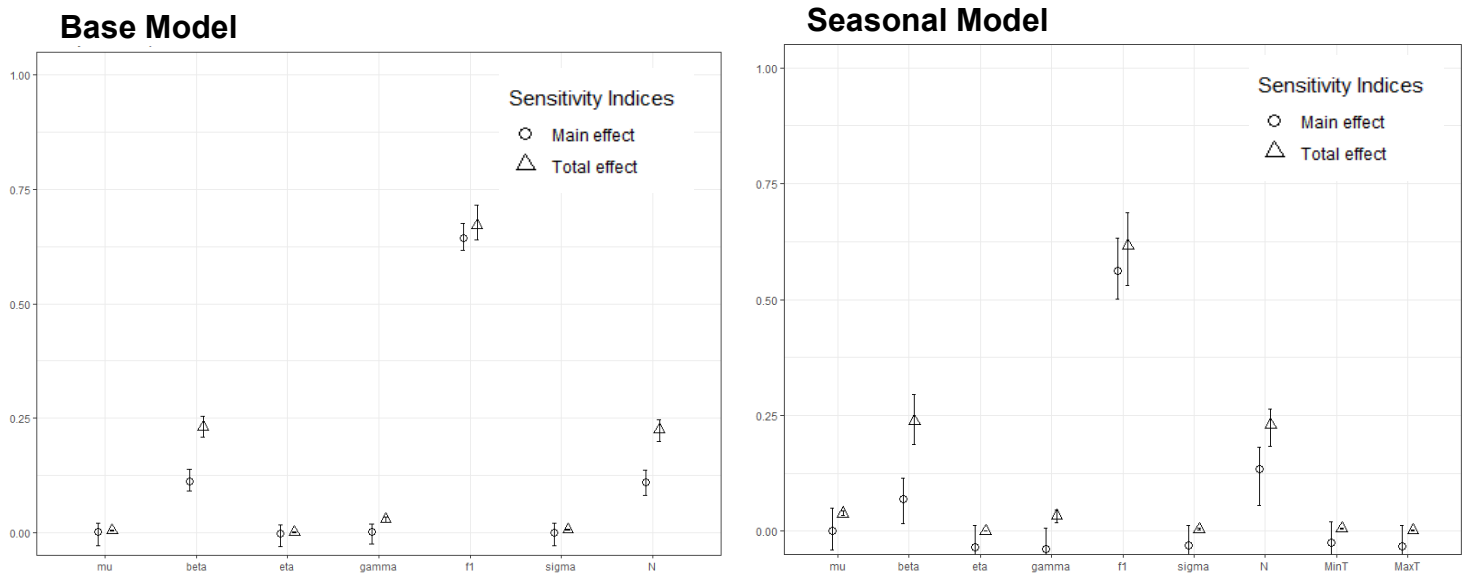

Figure 5 Global sensitivity analysis for base model (left) and seasonal model (right) of population suppression as a model output

5 Discussion and Conclusion

The strongest conclusion of the sensitivity analysis is that the fatality rate is a highly important factor in the resultant population after virus release. It is quite surprising for a single parameter to explain so much in the variance because it is a nonlinear model that is known to have threshold effects. Therefore further research should be directed towards exploring the ancestry of Australian carp, since genetic resistance could have significant impacts on the desired outcome of the virus release. Australian carp have large hereditary relations to European carp with some relation to Asian carp. There are four known strains that have been released into Australia - Yanco, Prospect, Boolara, and Japanese koi - and such hybridisation can be detrimental to control efforts and increase carp adaptability to new environments (Haynes, 2011). Therefore, genetic ancestry plays a vital role in the adaptability of Australian carp and is going to be a crucial component on the success of the biocontrol.

Another important observation is the similarity between the sensitivity analyses between both models. Epidemiological modelling has the ambition of reproducing observed data for reliable use of future predictions. However, it is possible to develop simple models, such as the base model, that can provide useful analytical results of the dynamic behaviour of disease in certain populations. While the reality is far more complex, the sensitivity analyses have shown that though the model

was extended, both the base and seasonal model had similar results. In future it would be noteworthy to conduct a GSA for the age structure model and possibly a more advanced model to examine whether the results will remain similar to the base model, demonstrating that sometimes a simple model can be a good model.

Acknowledgements

My completion of this project could not have been accomplished without the support of A/Prof Stephen Davis and Dr Jess Hopf. Their guidance and supervision throughout this project is greatly appreciated and I thank them for their encouragement to pursue research.

I would also like to thank RMIT University and AMSI for giving me the opportunity of being a part of this program.

Appendices

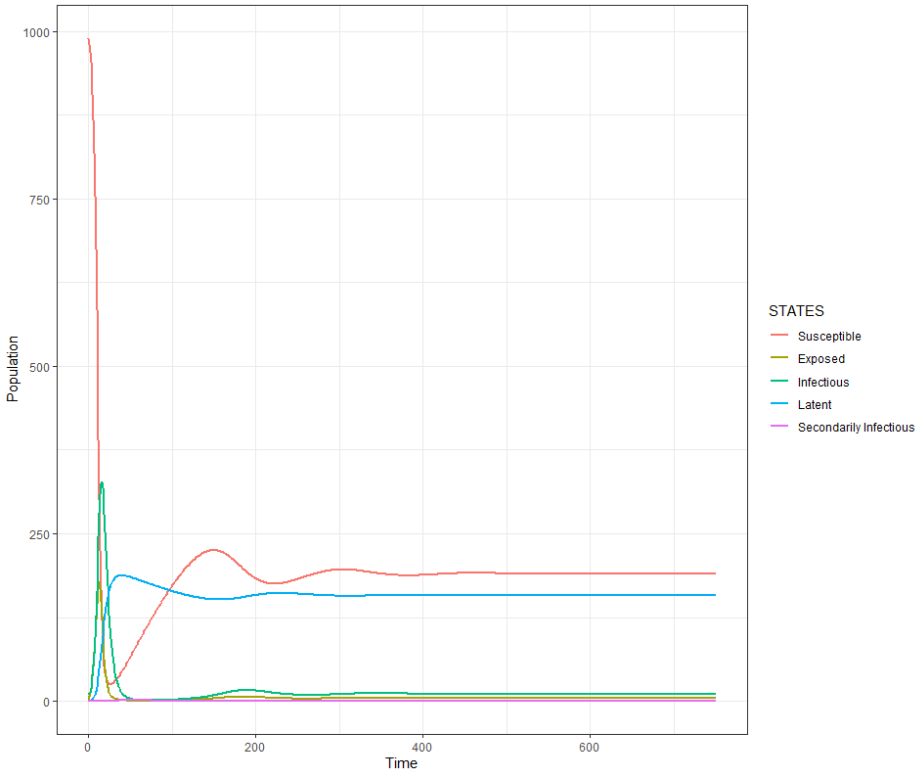

A 1 Epidemiological time series plot of the population size of each disease state of the base model. Disease dynamics only occur just after virus release and subsequently the population reaches equilibrium

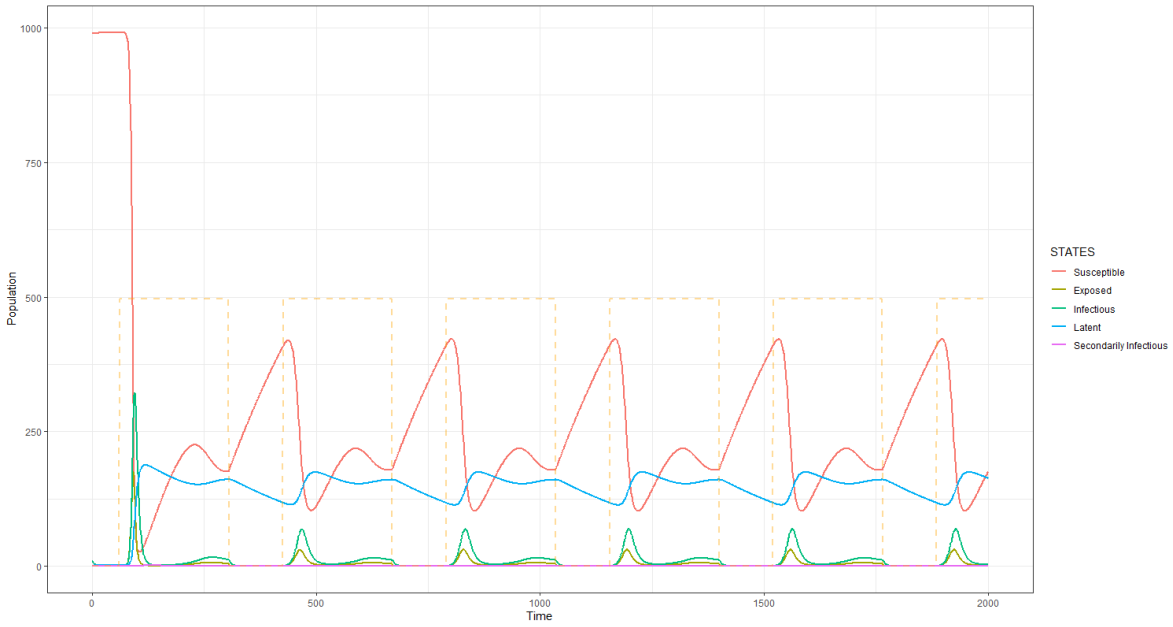

A 2 Epidemiological time series plot of the population size of each disease state for a model with temperature dependence. The plot clearly highlights seasonal dynamics, where successive disease state peaks stabilise and repeat. The largest outbreaks occur during spring with some small outbreaks in autumn, reflecting observational data.

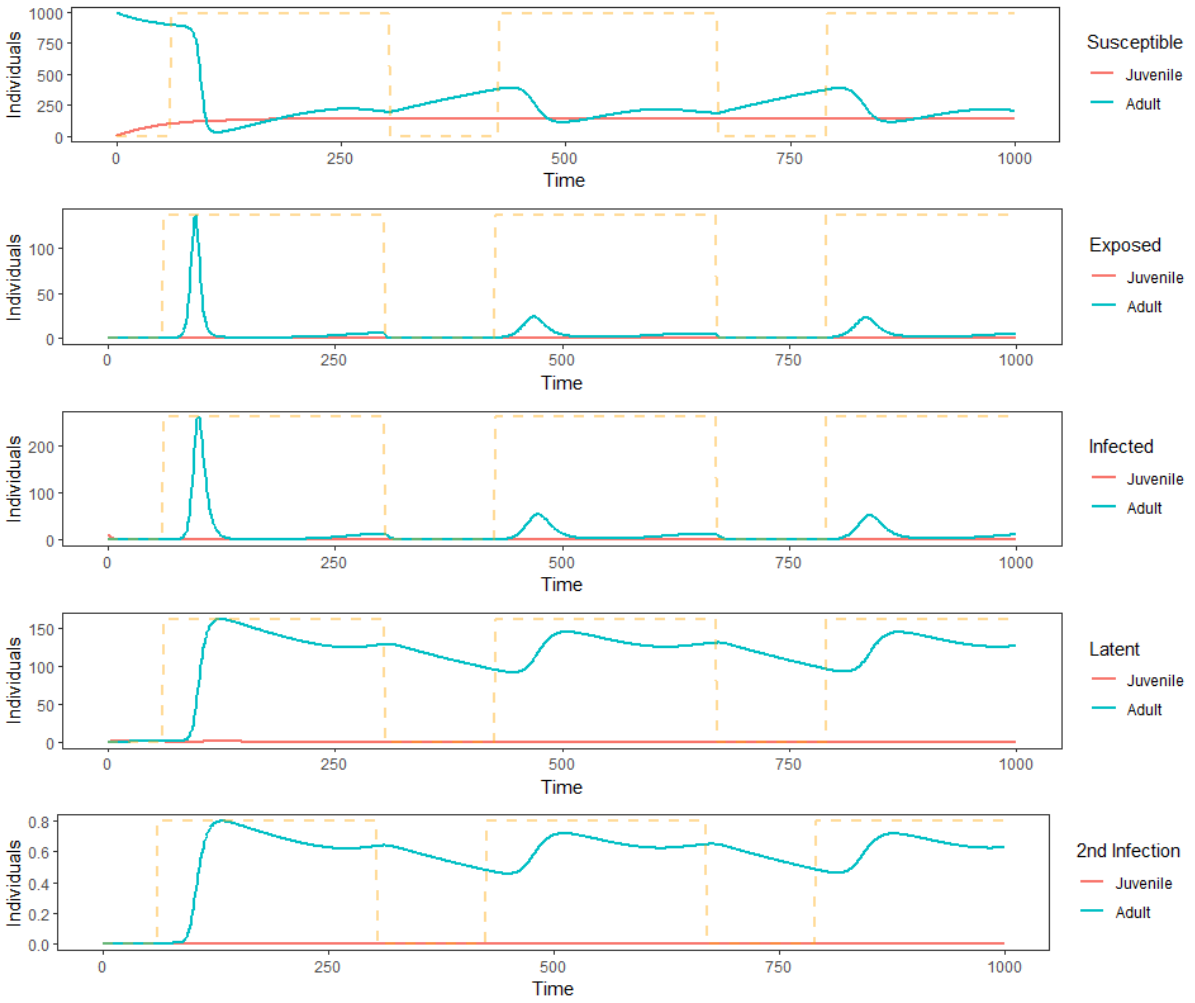

A 3 Epidemiological time series plot of the population size of juveniles and adults within each disease state where infectious peaks only occur within the adult population during spring.

References

[1] Davis, S. Hopf, J., Arakala1, A., McColl, K.A., Graham, K., and P.A. Durr, P.A. (2020) The predicted impact of Cyprinid herpesvirus 3 as a potential biocontrol agent for controlling invasive common carp (Cyprinus carpio) in Australia. RMIT University.

[2] Fao.org. (2020). FAO: Growth. [online] Available at: http://www.fao.org/fishery/affris/species-profiles/common-carp/growth/en/ [Accessed 9 Jan. 2020].

[3] Haas, K., Köhler, U., Diehl, S., Köhler, P., Dietrich, S., Holler, S., Jensch, A., Niedermaier, M. and Vilsmeier, J. (2007). Influence of fish on habitat choice of water birds: a whole-system experiment. Ecology 88, pp.2915–2925.

[4] Hanifie, S. (2020). Concerns over use of herpes virus in National Carp Control Plan. [online] ABC News. Available at: https://www.abc.net.au/news/2019-05-27/carp-control-plan-not-ready/11130326 [Accessed 26 Feb. 2020].

[5] Haynes, G. (2011). Carp: Habitat, Management and Disease. Chapter 3: Common Carp as Invasive Species. Carp: Habitat, Management and Disease.

[6] Matsuzaki, S., Usio, N., Takamura, N. and Washitani, I. (2009). Contrasting impacts of invasive engineers on freshwater ecosystems: an experiment and meta-analysis. Oecologia, 158, pp.673–686.

[7] McColl, K., Sunarto, A., Slater, J., Bell, K., Asmus, M., Fulton, W., Hall, K., Brown, P., Gilligan, D., Hoad, J., Williams, L. and Crane, M. (2016). Cyprinid herpesvirus 3 as a potential biological control agent for carp (Cyprinus carpio) in Australia: susceptibility of non-target species. Journal of Fish Diseases, 40(9), pp.1141-1153.

[8] Omori, R. and Adams, B. (2011). Disrupting seasonality to control disease outbreaks: The case of koi herpes virus. Journal of Theoretical Biology, 271(1), pp.159-165.

[9] Parkos, J. J. III, Santucci, V. J. Jr, and Wahl, D. W. (2003). Effects of adult common Carp (Cyprinus carpio) on multiple trophic levels in shallow mesocosms. Canadian Journal of Fisheries and Aquatic Sciences, 60, pp.182–192.

[10] Saltelli, A., Annoni, P., Azzini, I., Campolongo, F., Ratto, M. and Tarantola, S. (2010). Variance based sensitivity analysis of model output. Design and estimator for the total sensitivity index. Computer Physics Communications, 181(2), pp.259-270.

[10] Uchii, K., Minamoto, T., Honjo, M. and Kawabata, Z. (2013). Seasonal reactivation enables Cyprinid herpesvirus 3 to persist in a wild host population. FEMS Microbiology Ecology, 87(2), pp.536-542.

[11] Williams, A. E., Moss, B. and Eaton, J. (2002). Fish induced macrophyte loss in shallow lakes: top-down and bottom-up processes in mesocosm experiments. Freshwater Biology, 47, pp. 2216–2232.

[12] Yuasa, K., Ito, T. and Sano, M. (2008). Effect of Water Temperature on Mortality and Virus Shedding in Carp Experimentally Infected with Koi Herpesvirus. Fish Pathology, 43(2), pp.83-85.